JAGUAR PROCEDURES FOR DETONATION PROPERTIES OF ALUMINIZED EXPLOSIVES

Ernest L. Baker and Christos Capellos
U.S. ARMY TACOM-ARDEC
Picatinny Arsenal, New Jersey 07806

Leonard I. Stiel
Polytechnic University
Six Metrotech Center
Brooklyn, New York 11201

Improved relationships for the thermodynamic properties of solid and liquid aluminum and aluminum oxide for use with JAGUAR/Al thermochemical equation of state routines were developed in this study. Analyses of experimental melting temperature curves for aluminum and aluminum oxide indicated that improved coefficients were required for the volumetric relationships for the liquids. NLPQB optimization routines were utilized in conjunction with the experimental melting point data to establish improved volumetric coefficients for these substances. The resulting property libraries resulted in improved agreement with experimental Hugoniot data for a wide range of pressure. Detonation properties were calculated with JAGUAR/Al using the revised property libraries for the aluminized explosive, PAX-3. Constants of the JWLB equation of state were established for varying extent of aluminum reaction and were utilized for comparisons with experimental cylinder velocities for this explosive.

INTRODUCTION

Accurate analytical procedures (JAGUAR/Al) based on an advanced thermochemical equation of state have been developed in this study for the calculation of detonation properties of high-blast aluminized explosives. For H-C-N-O explosives, JAGUAR is an efficient and accurate computer program[1] which uses NLQPEB advanced variable metric optimization routines[2] to determine equilibrium compositions with optimally parameterized JCZ3 relationships. Input options include the calculation of C-J points, isentropes, and Hugoniot curves of explosives. The JAGUAR procedures enable the calculation of the detonation properties of explosives for wide ranges of temperatures and pressures, including overdriven conditions .[3,4]

In JAGUAR/Al, revised calculation procedures for detonation properties based on the minimization of the Gibbs free energy of the coexisting gas and condensed phases have been implemented. Relationships for the melting curves of aluminum and aluminum oxide have been applied in JAGUAR/Al and are used to identify the correct phases present for the calculations. It is essential that accurate relationships are available for the thermodynamic properties of these components to obtain reliable results. Therefore, in this study, improved property libraries have been developed for solid and liquid aluminum and aluminum oxide by analyses of experimental melting point and Hugoniot data.

MELTING CURVE FOR ALUMINUM

The recent data of Boehler and Ross[5] provides melting temperatures of aluminum to 0.6 Mbar. These data are consistent with previous aluminum melting point data[6,7] at lower pressures and temperatures. The experimental temperatures were correlated to the pressure by the following relationship:[5]

$$T_m = T_{mo}\left(\frac{P}{60.49}+1\right)^{0.531} \qquad (1)$$

where T_{mo}=933.45 K and P is in kbar.

In order to establish improved relationships for heat capacities and volumes of solid and liquid aluminum, melting pressures as functions of the temperature of the solid were determined through the relationship

$$\mu^l(T,P) = \mu^s(T,P) \qquad (2)$$

where μ is the chemical potential. For condensed species, the chemical potential is calculated as

$$\mu_i = \mu_i^o(T) + \int_{P^o}^{P} V_i(T,P)\,dP \qquad (3)$$

where P^o = 1 bar. The solid (i=1) or liquid (i=2) volume is represented as

$$V_i = A_{i1} + A_{i2}P + A_{i3}P^2 \qquad (4)$$

and

$$A_{i1} = a_{i1} + a_{i2}T + a_{i3}T^2 \qquad (5)$$

$$A_{i2} = a_{i4} + a_{i5}T + a_{i6}T^2 \qquad (6)$$

$$A_{i3} = a_{i7} + a_{i8}T + a_{i9}T^2 \qquad (7)$$

From Equations (3) and (4), the residual chemical potential (the integral term in Equation (3) is

$$\frac{\Delta\mu_i^*}{RT} = \frac{1}{RT}\left(A_{i1}P + \frac{A_{i2}}{2}P^2 + \frac{A_{i3}}{3}P^3\right) \qquad (8)$$

The chemical potential of the condensed phase at the reference pressure (1 bar) is calculated as

$$\frac{\mu^o{}_i}{RT} = \frac{H^o{}_i}{RT} - \frac{S^o{}_i}{R} \qquad (9)$$

The reference state enthalpies and entropies, H_i^o and S_i^o, are obtained from the standard heat capacities of the condensed components. The function utilized for the temperature variation of the heat capacities is of the form

$$\frac{C_{pi}^o}{R} = \sum_{j=0}^{3} c_{ij}\theta^j + \sum_{j=1}^{3} d_{ij}\theta^{(-j)} \qquad (10)$$

where θ = T (K)/1000.

An inspection of Equations (3)-(10) indicate that the calculated chemical potentials are sensitive to the values of $a_{i1}\ldots a_{i9}$ of Equations (5) - (7) for solid and liquid volumes and to the values of $c_{i0},\ldots c_{i3}$, and $d_{i1},..d_{i3}$ of Equation (10) for the heat capacities. Accurate coefficients of Equation (10) for heat capacities of solid aluminum for 298 – 933 K and for liquid aluminum from 933 – 2791 K were presented with the 1998 NIST-JANAF Thermochemical Tables[8].

In Figure 1, calculated values from the NIST relationship for solid aluminum are shown for the temperature range 300-1500 K. It can be seen that the extrapolated values from this relationship increase rapidly for temperatures above 933 K. The heat capacities from the BKWC relationship[9] for Equation (10) increase even more rapidly at elevated temperatures. In order to provide a more moderate extrapolation of the experimental solid heat capacities, the NIST values for temperatures to 933K were represented with good accuracy by the linear relationship

$$\frac{C_{p1}^o}{R} = 1.6021\theta + 2.4241 \qquad (11)$$

The NIST- JANAF heat capacities for liquid aluminum are constant at 31.75J/mole K for temperatures above 933 K. At lower temperatures the liquid heat capacities decrease rapidly, and it is difficult to represent the behavior for a wide temperature range with a single relationship of the form of Equation (10). The BKWC heat capacity relationship for liquid aluminum represents a good compromise for the entire temperature range.

Melting temperatures calculated with Equation (2) and the BKWC relationships for solid and liquid heat capacities and volumes are in good agreement with the experimental values at low pressure, but deviate at higher pressures, as shown in Figure 2. Melting pressures could not be calculated with these functions for pressures above 40 kbar. Similar behavior was observed by the use of the linear relationship, Equation (11), for solid heat capacities. An examination of available experimental data for liquid volume resulted in the following slightly revised relationship for the coefficients of Equation (5):

$$A_{21} = 10.278 + 0.00185T \qquad (12)$$

Figure 2 presents calculated and experimental melting curves for aluminum. The melting temperatures for aluminum calculated with Equation (11) for heat capacities of the solid, Equation (12) for A_{21}, and the BKWC relationships for the other heat capacity and volume coefficients are higher than the experimental temperatures at intermediate pressures. They are substantially lower than the experimental temperatures at high pressures (REVISED BKWC).

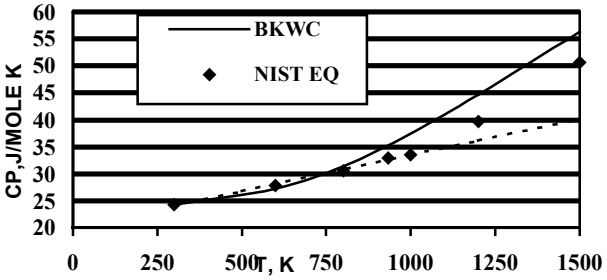

FIGURE 1. HEAT CAPACITY OF AL(S)

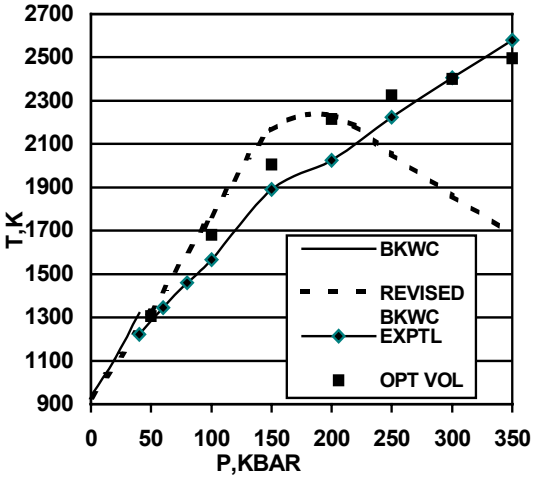

FIGURE 2. MELTING CURVE OF ALUMINUM

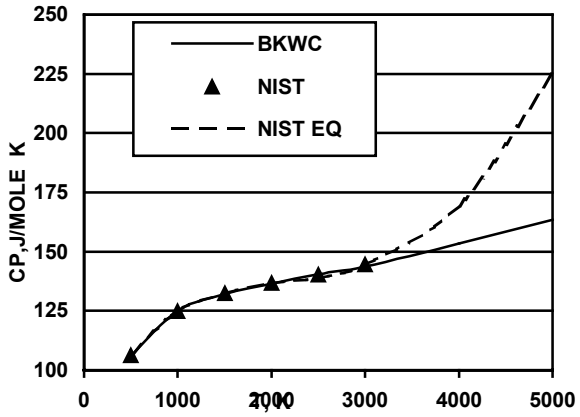

FIGURE 3. HEAT CAPACITY OF ALUMINUM OXIDE (s)

It has been found that the calculated melting point curve is quite sensitive to the temperature and pressure variation of the calculated liquid volumes. Therefore, the NLQPEB nonlinear optimization routines developed by Baker[2] were utilized to establish improved coefficients a_{24}, a_{25}, a_{27} and a_{28} of the linear and quadratic terms in pressure for the liquid volume, Equations (6) and (7), with a_{26} and a_{29} =0. The following objective function was utilized for seven pressures in the range 50 –350 kbar:

$$Z = \frac{\sum_j \left(T_j - TX_j\right)^2}{N} \qquad (13)$$

where T is the temperature calculated with Equation (2) at pressure P and TX is the corresponding experimental temperature from Equation (1). For these studies Equation (11) was used for the solid heat capacity, and the BKWC coefficients for solid volume were modified slightly based on the analysis of experimental Hugoniot data for solid aluminum. The BKWC liquid heat capacity relationship was utilized along with the coefficients of Equation (12) for a_{21} and a_{22} for the liquid volume.

The calculated melting point temperatures with the optimized liquid volumetric coefficients of Equations (6) and (7) are shown in Figure 2 to be in good agreement with the experimental values for pressures to 350 kbar. The revised coefficients for aluminum volumes to be utilized with JAGUAR/Al are presented in Table 1. The corresponding heat capacity coefficients are in Table 2.

MELTING CURVE FOR ALUMINUM OXIDE

A similar analysis was performed for the thermodynamic properties and melting point curve of aluminum oxide. In Figure 3, heat capacities from the BKWC relationship for solid aluminum oxide are seen to be in good agreement with the values from the NIST-JANAF relationship[8] for the range of the experimental data (298-2327 K). However the extrapolated heat capacities for elevated temperatures show a more reasonable increase for the BKWC relationship than the sharp rise exhibited with the NIST coefficients. The NIST-JANAF liquid heat capacities for aluminum oxide are constant at 192.5 J/mole K for temperatures from 2327-4000 K. The BKWC relationship for this property provides a reasonable compromise to represent both the constant high temperature values and the rapid decrease of this property at low temperatures.

TABLE 1. COEFFICIENTS OF VOLUME RELATIONSHIPS

	SOLID Al	**LIQUID Al**	**SOLID Al2O3**	**LIQUID Al2O3**
ai1	**9.704**	**10.278**	**25.54**	**54.14**
ai2	**9.19E-4**	**1.1185E-3**	**.4691E-3**	**-.7156E-2**
ai3	**0**	**-.824E-5**	**0**	**0**
ai4	**-.922E-5**	**-.5292E-8**	**-.871E-5**	**.5714E-5**
ai5	**-.95E-9**	**0**	**0**	**-1.01E-11**
ai6	**0**	**0**	**0**	**0**
ai7	**0**	**.5936E-11**	**.353E-11**	**0**
ai8	**0**	**.5747E-14**	**0**	**0**
ai9	**0**	**0**	**0**	**0**

TABLE 2. COEFFICIENTS OF EQUATION (10)

	SOLID Al	LIQUID Al	SOLID Al2O3	LIQUID Al2O3
ci0	2.4241	4.3578	19.788	62.719
ci1	1.6021	-0.4447	-1.636	-8.667
ci2	0	0.1143	.5304	.3384
ci3	0	-0.00932	-0.03522	.04633
di1	0	0.1907	-4.2187	-60.912
di2	0	-.5284	.72055	26.631
di3	0	0.1058	-.1008	-3.874

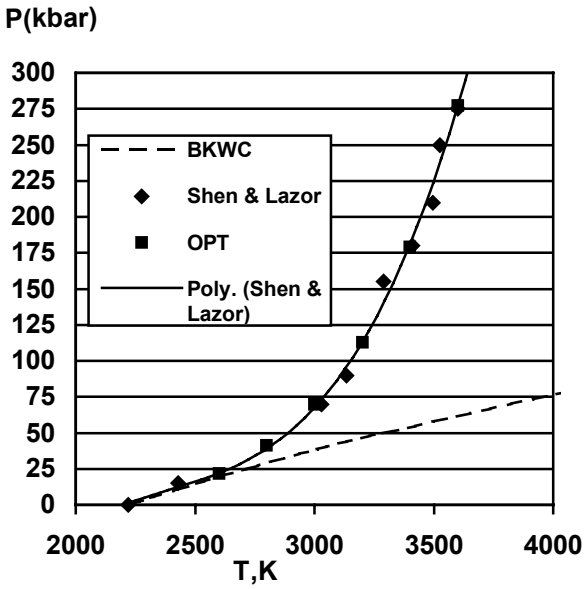

FIGURE 4.ALUMINUM OXIDE MELTING CURVE

Melting temperature measured by Shen and Lazor[10] for aluminum oxide for pressures to 275 kbar are presented in Figure 4. The experimental data were represented in this study by the following polynomial relationship:

$$P(kbar) = 115.34\theta^3 - 825.54\theta^2 + 2019.4\theta - 1674.9 \quad (14)$$

It can be seen in Figure 4 that the melting temperatures calculated with Equation (2) and the BKWC relationships for thermodynamic properties of solid and liquid aluminum oxide are substantially lower than the experimental values.

The NLQPEB optimization routines were utilized to develop improved coefficients of the liquid volumetric relationship, Equations (4) - (7) for aluminum oxide. The coefficients a_{21}, a_{22}, a_{24}, and a_{25} were established with the other volumetric coefficients equal to zero. The objective function for this case was

$$Z = \frac{\sum_j \left(P_j - PX_j\right)^2}{N} \quad (15)$$

where P_j is the calculated pressure from Equation (2) for temperatures in the range 2600-3600 K, and PX_j is the corresponding experimental value from Equation (14).

It can be seen from Figure 4 that the calculated pressures with the optimized liquid volume relationship are in good agreement with the experimental values for the entire range to 300 kbar. The new aluminum oxide property coefficients from this study are presented in Tables 1 and 2.

COMPARISONS WITH HUGONIOT DATA

The revised property libraries for aluminum and aluminum oxide were utilized to compare the resulting Hugoniot curves with experimental data. The Newton-Raphson iteration method was used to find the Hugoniot temperature and corresponding specific volume at a specified pressure P through the function

$$FX = P - P_C = f(T) \quad (16)$$

The calculated pressure P_C results from an energy balance along the Hugoniot curve for the explosive as

$$P_C = 2\left(\frac{e - e_R}{v_R - v}\right) - P_R \quad (17)$$

where e is the specific energy of the solid or liquid component and e_R is the reference internal energy at the initial conditions P_R and v_R. At each iteration of temperature, melting pressures were calculated from Equation (1) for aluminum and Equation (14) for aluminum oxide. If the calculated melting pressure is higher than the pressure P, then the properties for the liquid state are used. Otherwise the heat capacity and volumetric coefficients are for the solid. In some cases the iterations were indicated to be close to the phase boundary and convergence was difficult.

In Figure 5, calculated Hugoniot reduced volumes $V^*=v/v_R$ for aluminum are shown to be in good agreement with experimental values[11] for v_R=0.520 cm^3/g and pressures from 175 to 525 kbar. The states for the calculated points are indicated to be solid at low pressures, liquid at the highest pressures, and close to the phase boundary at intermediate pressures. The volumes calculated with the original BKWC property relationships are considerably higher than the experimental values for the entire pressure range.

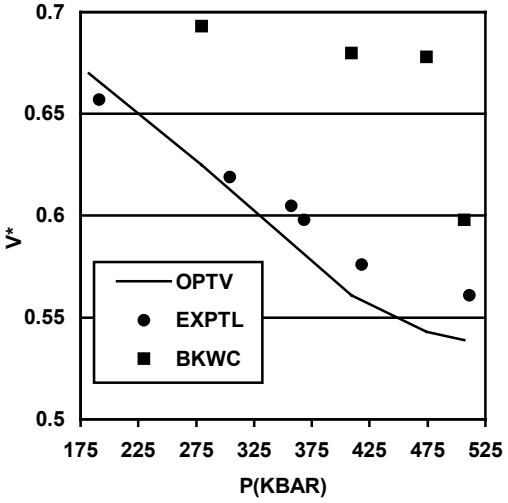

FIGURE 5. V* VS P FOR Al (RHO=1.923 g/cc)

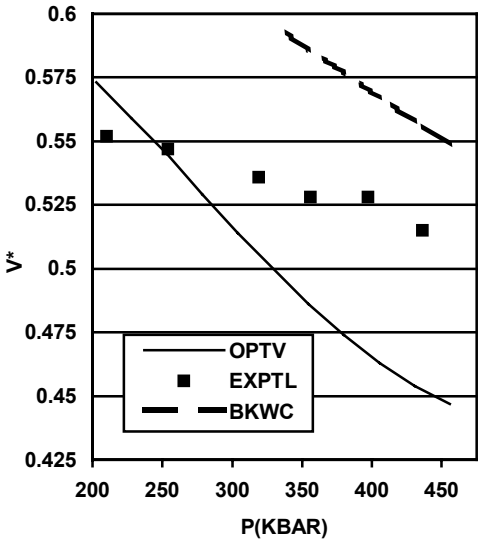

FIGURE 6. V* VS P FOR Al (RHO=1.587 g/cc)

Similar comparisons are shown in Figure 6 for aluminum Hugoniot data[11] in the range 200 – 450 kbar for v_R=0.630 cm^3/g. The calculated states are for the liquid for the entire range. The calculated Hugoniot volumes are in reasonable agreement with the experimental values to about 300 kbar, but are lower at higher pressures. The indicated Hugoniot temperatures are as high as 5000 K at the highest pressure. The volumes calculated with the BKWC property relationships are higher than the experimental values for the entire range.

Calculated Hugoniot values for aluminum (v_R = 0.741) are compared in Figure 7 with experimental data (10) for pressures in the range 175-375 kbar. At every point the calculated states are indicated to be liquid by Equation (1). For most of the range the calculated volumes decrease more rapidly with pressure than the experimental values. The temperatures for the calculated Hugoniot points are as high as 6000 K at the highest pressure. The calculated volumes with BKWC coefficients for all properties are higher than the experimental points.

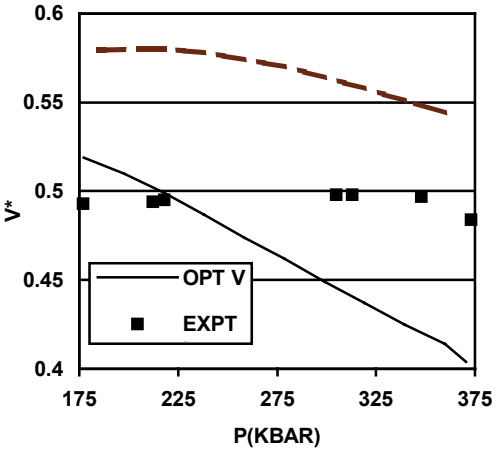

FIGURE 7. V* VS P FOR Al (RHO=1.35 g/cc)

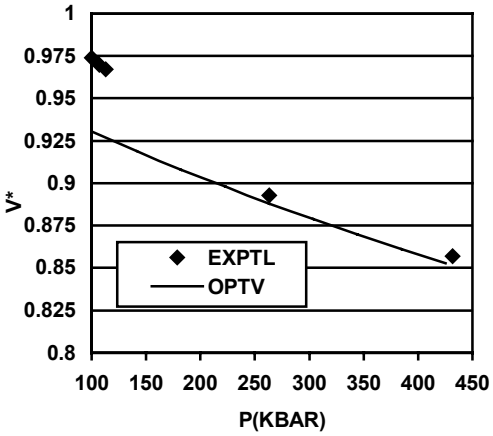

FIGURE 8. V* VS P FOR Al OXIDE (RHO=3.812 g/cc)

In Figure 8 calculated Hugoniot volumes for aluminum oxide (v_R = 0.262) are seen to be in reasonable agreement with experimental values[12] for pressures for 100-450 kbar. The equilibrium state is for the solid at all points in this range, and the temperature varied from 379-745K. Identical results were obtained with the BKWC library since the BKWC coefficients for solid properties were utilized for aluminum oxide.

JWLB PROCEDURES FOR ALUMINIZED EXPLOSIVES

In JAGUAR/Al the equilibrium composition of the explosive products is established by the minimization of the Gibbs free energy of the composite system at fixed T and P. The procedures enable the calculation of detonation properties at specified T, P points, for Hugoniot curves, at the C-J condition, and for isentropic expansions. A default freeze temperature of 2200 K has been found to be most suitable for the JCZ3 equation of state with optimized parameters.

In JAGUAR/Al the parameters of the JWLB equation of state[13] are established for aluminized explosives from the calculated thermodynamic properties for the principal isentrope. The FIT option utilizes the NLQPEB variable metric optimization routines to parameterize the following relationships for each explosive:

$$\lambda = \sum_i (A_{\lambda i} V^* + B_{\lambda i}) e^{-R_{\lambda i} V^*} + \omega \qquad (18)$$

$$P_s = \sum_i A_i e^{(-R_i V^*)} + C V^{*-(\omega+1)} \qquad (19)$$

where λ is the Gruneisen parameter, V* the relative expansion volume, and P_s the isentrope pressure. Numerical procedures are employed to obtain values of λ along the principal isentrope from the relationship

$$\lambda = \frac{T}{V}\left(\frac{\partial V}{\partial T}\right)_S \approx \frac{T}{V}\left(\frac{\Delta V}{\Delta T}\right)_S \qquad (20)$$

In a standard run overdriven points are included and calculations are performed for the principal isentrope at 110 points for pressures from 500 to 0.005 kbar.

For the isentropic P-V* relationship, Equation (6), the A_i, R_i, and C variables are constrained to be positive, and the C-J pressure and detonation velocity resulting from the JWLB relationship are constrained to be equal to the calculated values. In order to obtain optimum accuracy for the important region of high expanions, the detonation energies at V*≈ 7 and at 5 bar pressure are also constrained so that the JWLB and JAGUAR/Al values are equal. In addition, since the JCZ3 relationships may not be accurate at low pressures and temperatures, for pressures below 250 bar the properties of the gaseous mixture are established with the Peng-Robinson equation of state[14] which is of a revised van der Waals form:

$$P = \frac{RT}{v-b} - \frac{a(T)}{v(v+b)+b(v-b)} \qquad (21)$$

CALCULATION OF DETONATION PROPERTIES FOR PAX3

The revised property libraries (Tables 1 and 2) for aluminum and aluminum oxide were incorporated into the JAGUAR/Al thermochemical equation of state routines for the calculation of the detonation properties of explosives. Equations (1) and (14) are utilized to establish the proper equilibrium states for each point calculation.

Detonation properties were calculated for a PAX-3 explosive with 66% HMX, 15.9% plasticizer, and 18.1% aluminum by weight (ρ_o=1.866) and compared with available experimental information from full-wall cylinder test measurements conducted at Picatinny Arsenal with a one inch cylinder for this formulation. Varying fractions of reacted and unreacted aluminum were considered. In Figure 9 the C-J velocity is shown to decrease only slightly with increasing fraction of aluminum reacted. However, as shown in Figure 10 the calculated detonation energies for PAX-3 at V* = 7 are much more negative for increasing fraction of reacted metal. The limiting detonation energy E_o is also seen to exhibit similar behavior for these systems. Therefore the extent of reaction for an aluminized explosive formulation can be accurately established from experimental cylinder velocities and corresponding detonation energies with JAGUAR/Al calculations.

Constants of the JWLB relationships, Equations (18) and (19), for the principal isentrope were also established or PAX3 for varying percentages of aluminum reaction. The JWLB constants and related information are presented

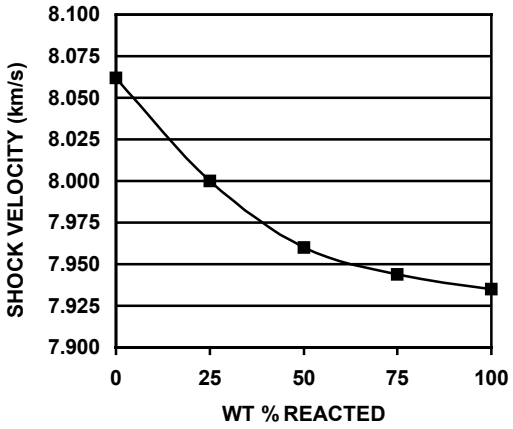

FIGURE 9 C-J VELOCITY FOR PAX-3

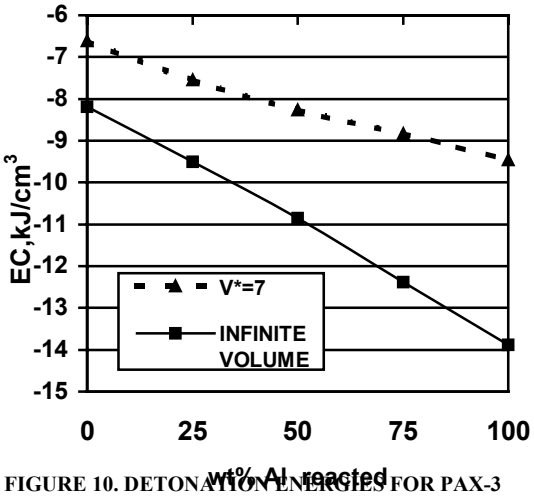

FIGURE 10. DETONATION ENERGIES FOR PAX-3

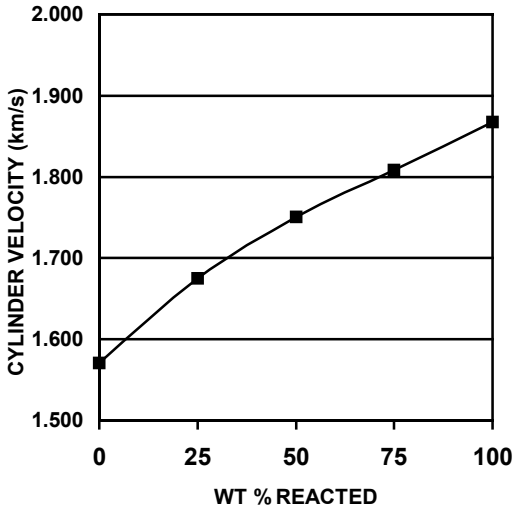

FIGURE 11. CYLINDER VELOCITY PAX-3

Table 3. JWLB Parameters for PAX-3 (18.1 wt% Al)

	WEIGHT FRACTION OF Al REACTED				
	0%	25%	50%	75%	100%
ρ0 (g/cc)	1.866	1.866	1.866	1.866	1.866
E0 (kJ/cm^3)	-8.189	-9.509	-10.856	-12.376	-13.881
*D*CJ (cm/μs)	0.8062	0.79965	0.9602	0.79439	0.79354
*P*CJ (Mbar)	0.2956	0.2960	0.29836	0.30095	0.30068
A1 (Mbar)	452.049	347.626	452.115	518.918	203.135
A2 (Mbar)	5.40863	8.74604	4.84063	2.80141	108.703
A3 (Mbar)	0.147902	1.0165	0.798616	0.941623	1.78819
A4 (Mbar)	0.160397	0.75125	0.547288	0.424729	0.078905
R1	13.7049	13.4009	13.3332	13.3243	11.2904
R2	4.37003	5.80061	4.90189	4.78731	18.2708
R3	2.61455	17.7697	8.51967	3.69231	2.95849
R4	1.51048	2.0915	1.8683	1.73909	1.04924
C (Mbar)	0.007799	0.009655	0.011415	0.013449	0.014608
ω	0.283973	0.283286	0.263909	0.238574	0.216557

in Table 3 for this PAX-3 composition and varying percentages of reacted aluminum.

The constants of Equations (18) and (19) were utilized to calculate cylinder expansion velocities with an analytic cylinder test model[2]. Previous comparisons with DYNA2D calculations have shown that the analytical cylinder model is accurate at 7 inside expansion volumes. In Figure 11 the resulting cylinder velocities are seen to vary sensitively with the extent of aluminum reaction. The experimental velocity at seven area expansions is 1.539-1.567 km/s. For 0% aluminum reaction the corresponding calculated cylinder velocity is 1.571 km/s. A comparison with the values of Figure 10 indicate that incomplete reaction has resulted for this sample to seven area expansions. The experimental C-J velocity for this sample is 7.957 km/s, while the calculated value for 0% aluminum reaction is 8.061, a difference of 1.3%. The agreement for both calculated C-J velocity and cylinder velocity with the improved aluminum and aluminum oxide libraries of this study is considerably better than obtained with the BKWC libraries. Calculations with CHEETAH 2.0 and 3.0 also indicate that the aluminum is largely unreacted over this expansion range**.**

DISCUSSION

The revised property libraries for aluminum and aluminum oxide developed in this study result in substantially improved agreement for the variation of the melting point temperatures for wide ranges of pressure for aluminum and aluminum oxide. The accurate calculation of melting points is essential to enable the correct identification of the equilibrium states and to determine reliable detonation properties with the JAGUAR/Al routines.

The revised libraries were found to result in improved agreement with experimental Hugoniot data for aluminum liquid states at low initial densities and high Hugoniot temperatures. Further improvement can possibly be obtained by extending the optimization studies for the melting curve of aluminum to higher temperatures.

The revised libraries developed in this study enable consistent results for detonation properties with the JAGUAR/Al thermochemical equation of state routines. For a PAX-3 explosive formulation more consistent agreement with experimental C-J and detonation velocities resulted with the revised aluminum and aluminum oxide properties.

LITERATURE CITED

1. Stiel. L.I., *Optimized JCZ3 Procedures for Detonation Energies of Explosives,* Final Report Contract NO. DAAL03-91-C-0034, TCN No. 956120, Picatinny Arsenal, NJ, October, 1996.

2. Baker, E.L., *Modeling and Optimization of Shaped Charge Liner Collapse and Jet Formation*, ARAED-TR-92019, Picatinny Arsenal, NJ, January 1993.

3. Stiel, L.I., and Baker, E.L., "Detonation Energies of Explosives by Optimized JCZ3 Procedures", *Proceedings of 1997 APS Topical Conference of Condensed Matter*, Amherst, MA., August, 1997.

4. Stiel, L.I., and Baker, E.L., Optimized JCZ3 Procedures for Detonation Properties at Highly Overdriven Conditions", *Proceedings of 1999 APS Topical Conference of Condensed Matter*, Snowbird, Utah, August, 1999.

5. Boehler, R., and Ross, M., "Melting Curve of Aluminum in a Diamond Cell to 0.8Mbar: Implications for Iron", *Earth and Planetary Science Letters*, 153, pp 223-227,1997.

6. Lees, J., and Williamson, B.H.J., "Combined very High pressure/High Temperature Calibration of the Tetrahedral Anvil Apparatus, Fusion Curves of Zinc, Alyminum, Germanium, and Silicon to 60 Kilobars", *Nature*, 208, pp. 278-279, 1965.

7. Jayarman,A., Klement, W., Newton, R.C., Kennedy, G.C., "Fusion Curves and Polymorphic Transitions of the Group III Elements-Aluminum, Gallium, Indium, and Thallium-at High Pressures", J. Phys. Chem. Solids, 24, pp 7-18, 1963.

8.Chase, M.W., Jr., "NIST- *JANAF Thermochemical Tables Fourth Edition"*, J. Phys. Chem. Ref. Data, Monograph 9, pp . 1-1951,1998.

9. Fried, L.E., Howard, M.W., and Souers, P.C., " *CHEETAH 2.0 User's Manual*", August, 1998.

10. Shen, G., and Lazor, P., "Measurement of Melting Temperatures of Some Minerals Under Lower Mantle Pressures", *J. Geophys. Res*., 100 (B9), pp. 17,699-17,713, 1995.

11. Anderson, G.D., Doran, D.G., and Fahrenbruch, A.L., Air Force Weapons Lab. Report:, AFWL-TR-65-147 , 1965.

12. Ahrens, T.J., Gust, W.H., and Royce, E.B., "Material Srength Effect in the Shock Compression of Alumina", *J. Appl. Phys*., 39, pp. 4610-4616, 1968.

13. Baker, E. L., "An Application of Variable Metric Nonlinear Optimization to the Parameterization of an Extended Thermodynamic Equation of State", *Proceedings of the Tenth International Detonation Symposium*, Boston. MA, pp. 394-400, July, 1993.

14. Peng, D.-Y, and Robinson, D.B., "A New Two-Constant Equation of State", *Ind. Eng. Chem. Fundamen.*, 15, pp. 59-64, 1976.

ACKNOWLEDGMENTS

L.I. Stiel's participation was supported by the TACOM Research, Development and Engineering Center (Mr. William Poulos) under the auspices of the U.S. Army Research Office Scientific Services Program administered by Battelle (Delivery Order 757, Contract No. DAAHO4-96-C-0086).